

# Probing the Mechanism of O<sub>2</sub> Activation by a Copper(I) Biomimetic Complex of a C–H Hydroxylating Copper Monooxygenase

Albert Poater\* and Luigi Cavallo

Dipartimento di Chimica, Università degli Studi di Salerno, via Ponte don Melillo, Fisciano (SA) 84084, Italy

Received November 26, 2008

In this paper, we report, for the first time, a plausible full reaction pathway for the activation of O<sub>2</sub> by a tetraazamacrocyclic monocopper(I) complex and for the subsequent intramolecular alkyllic hydroxylation to yield the alkoxide product. This theoretical insight offers remarkable support to the fundamental hypothesis in the field that a hydroperoxo complex of the type Cu<sup>I</sup>OOH intermediate is the key intermediate in this class of reactions. Overall, we give insight into an intramolecular alkyllic C–H bond activation due to the O<sub>2</sub> binding to copper(I) with an end-on  $\eta^1$ -O<sub>2</sub> ligation. The loss of a water molecule involves the final substrate oxygenation. The complex we consider is a biomimetic of several systems of biological relevance, such as amine oxidases, peptidylglycine- $\alpha$ -hydroxylating monooxygenase, and dopamine- $\beta$  monooxygenases.

## Introduction

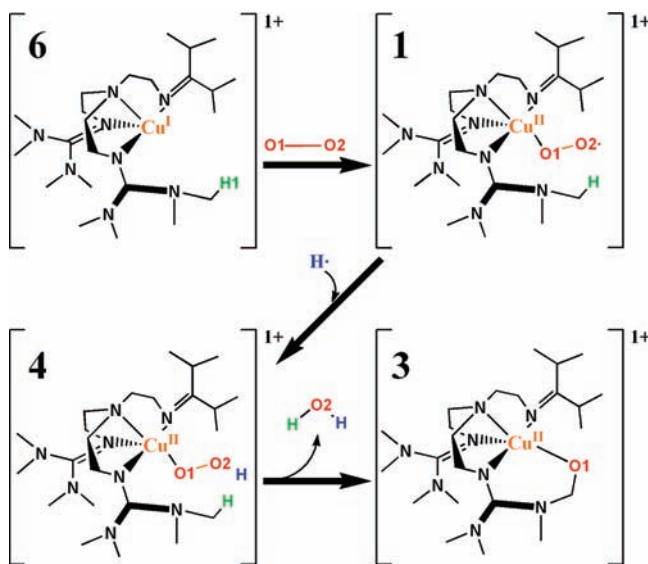
In efforts to gain a mechanistic understanding of the binding and activation of O<sub>2</sub> by a single copper ion in biological systems,<sup>1</sup> such as amine oxidases, peptidylglycine- $\alpha$ -hydroxylating monooxygenase (PHM),<sup>2,3</sup> and dopamine- $\beta$  monooxygenases (D $\beta$ M),<sup>2b,4</sup> a challenging field is still to gain insight into the nature of these intermediates.<sup>5</sup> For example, comprehension of the stability and reactivity of cores like Cu<sup>II</sup>O<sub>2</sub>,<sup>2,5c,6</sup> Cu<sup>II</sup>OOH,<sup>5a,7</sup> and Cu<sup>II</sup>O<sup>•5a,8</sup> is still incomplete, especially of the mechanisms in which they are involved. Nevertheless, identification of end-on  $\eta^1$ -O<sub>2</sub> ligation for a Cu<sup>II</sup>(O<sub>2</sub><sup>−</sup>) species has been possible through stopped-flow kinetic experiments or characterization at very low temperatures,<sup>9</sup> while Schindler and Sundermeyer obtained

the first X-ray structure with a Cu<sup>II</sup>(O<sub>2</sub><sup>−</sup>) core.<sup>9f</sup> Furthermore, besides the X-ray structure of PHM,<sup>3</sup> recent studies of Karlin et al. confirmed H-atom abstraction as a key step.<sup>10</sup>

On the reactive side, end-on superoxo Cu<sup>II</sup> species can promote oxygenation or oxidation of phenols,<sup>12</sup> but the details of this transformation are not completely understood yet, despite a recent publication of Solà et al. giving significant theoretical insight.<sup>13</sup> Very recently, Karlin et al. demonstrated that the cupric superoxide [Cu<sup>II</sup>(TMG<sub>3</sub>tren)- $\eta^1$ O<sub>2</sub><sup>•−</sup>]<sup>+</sup> species [**1**; TMG<sub>3</sub>tren = tris[(2-(N-tetramethylguanidyl)ethyl]amine] can also react with phenolic substrates to give a variety of oxidized, oxygenated, or hydroperoxylated products.<sup>10</sup> They also evidenced that the same substrates promote C–H activation and O-atom insertion, which involves an N-methyl group of the TMG<sub>3</sub>tren ligand of **1**, leading to the copper(II) alkoxide species **3**. This discovery corroborated the hypothesis that the first step of C–H hydroxylation involves H<sup>•</sup> abstraction to form a Cu<sup>II</sup>OOH species such as **4** of Scheme 1.<sup>10,12b</sup> One of the key experiments to strengthen this hypothesis has been the reaction of **1** with TEMPO-H, which is an excellent H<sup>•</sup> donor that is not prone to further reaction. The almost quantitative conversion of **1** into **3** in the presence of TEMPO-H strongly indicated the formation of the Cu<sup>II</sup>OOH species **4** as a key intermediate.<sup>10,12b</sup> In this paper, we provide complementary support to this key hypothesis by a full theoretical characterization of the conversion of **1** into **3**, in the presence of

\* To whom correspondence should be addressed. E-mail: albert.poater@udg.edu.

- (1) Halcrow, M. A. In *Comprehensive Coordination Chemistry II*; McCleverty, J. A., Meyer, T. J., Eds.; Elsevier: Amsterdam, The Netherlands, 2004; Vol. 8, pp 395–436.
- (2) (a) Prigge, S. T.; Mains, R. E.; Eipper, B. A.; Amzel, L. M. *Cell. Mol. Life Sci.* **2000**, *57*, 1236–1259. (b) Klinman, J. P. *Chem. Rev.* **1996**, *96*, 2541–2562. (c) Klinman, J. P. *J. Biol. Chem.* **2006**, *281*, 3013–3016.
- (3) (a) Prigge, S. T.; Eipper, B.; Mains, R.; Amzel, L. M. *Science* **2004**, *304*, 864–867. (b) Prigge, S. T.; Kolhekar, A. S.; Eipper, B. A.; Mains, R. E.; Amzel, L. M. *Science* **1997**, *278*, 1300–1305. (c) Prigge, S. T.; Kolhekar, A. S.; Eipper, B. A.; Mains, R. E.; Amzel, L. M. *Nat. Struct. Biol.* **1999**, *6*, 976–983.
- (4) Stewart, L. C.; Klinman, J. P. *Annu. Rev. Biochem.* **1988**, *57*, 551–592.

Scheme 1.<sup>11</sup>

TEMPO-H,<sup>14</sup> using the hybrid B3LYP density functional.<sup>15</sup> We will show that this transformation is energetically very facile. Thus, for the first time, we report a plausible full reaction pathway for the activation of O<sub>2</sub> by a tetraazamac-

- (5) (a) Itoh, S. *Curr. Opin. Chem. Biol.* **2006**, *10*, 115–122. (b) Gherman, B.; Heppner, D.; Tolman, W.; Cramer, C. J. *J. Biol. Inorg. Chem.* **2006**, *11*, 197–205. (c) Chen, P.; Solomon, E. I. *Proc. Natl. Acad. Sci. U.S.A.* **2004**, *101*, 13105–13110. (d) Quant Hatcher, L.; Karlin, K. D. *J. Biol. Inorg. Chem.* **2004**, *9*, 669–683. (e) Maiti, D.; Lee, D.-H.; Narducci Sarjeant, A. A.; Pau, M. Y. M.; Solomon, E. I.; Gaoutchenova, K.; Sundermeyer, J.; Karlin, K. D. *J. Am. Chem. Soc.* **2008**, *130*, 6700–6701. (f) Aboeella, N. W.; Gherman, B. F.; Hill, L. M. R.; York, J. T.; Holm, N.; Young, V. G., Jr.; Cramer, C. J.; Tolman, W. B. *J. Am. Chem. Soc.* **2006**, *128*, 3445–3458. (g) Reynolds, A. M.; Gherman, B. F.; Cramer, C. J.; Tolman, W. B. *Inorg. Chem.* **2005**, *44*, 6989–6997. (h) Maiti, D.; Narducci Sarjeant, A. A.; Karlin, K. D. *J. Am. Chem. Soc.* **2007**, *129*, 6720–6721. (i) Cramer, C. J.; Gour, J. R.; Kinal, A.; Wloch, M.; Piecuch, P.; Shahi, A. R. M.; Gagliardi, L. *J. Phys. Chem. A* **2008**, *112*, 3754–3767. (j) Rolff, M.; Tuczek, F. *Angew. Chem., Int. Ed.* **2008**, *47*, 2344–2347. (k) Malmqvist, P. A.; Pierlot, K.; Shahi, A. R. M.; Cramer, C. J.; Gagliardi, L. *J. Chem. Phys.* **2008**, *128*, 204109–10. (l) Raab, V.; Kipke, J.; Burghaus, O.; Sundermeyer, J. *Inorg. Chem.* **2001**, *40*, 6964–6971. (m) Gherman, B. F.; Tolman, W. B.; Cramer, C. J. *Comput. Chem.* **2006**, *27*, 1950–1961. (n) Aboeella, N. W.; Lewis, E. A.; Reynolds, A. M.; Brennessel, W. W.; Cramer, C. J.; Tolman, W. B. *J. Am. Chem. Soc.* **2002**, *124*, 10660–10661. (o) Aboeella, N. W.; Kryatov, S. V.; Gherman, B. F.; Brennessel, Young, V. G., Jr.; Sarangi, R.; Rybak-Akimova, E. V.; Hodgson, K. O.; Hedman, B.; Solomon, E. I.; Cramer, C. J.; Tolman, W. B. *J. Am. Chem. Soc.* **2004**, *126*, 16896–16911. (p) Spencer, D. J. E.; Aboeella, N. W.; Reynolds, A. M.; Holland, P. L.; Tolman, W. B. *J. Am. Chem. Soc.* **2002**, *124*, 2108–2109. (q) Chen, P.; Root, D. E.; Campochiaro, C.; Fujisawa, K.; Solomon, E. I. *J. Am. Chem. Soc.* **2003**, *125*, 466–474. (r) Piquemal, J.-P.; Pillemé, J.; Parisel, O.; Gérard, H.; Fourré, I.; Bergès, J.; Gourlaouen, C.; de la Lande, A.; Van Severen, M.-C.; Silvi, B. *Int. J. Quantum Chem.* **2008**, *108*, 1951–1969. (s) de la Lande, A.; Parisel, O.; Gérard, H.; Moliner, V.; Reinaud, O. *Chem.—Eur. J.* **2008**, *14*, 6465–6473. (t) de la Lande, A.; Gérard, H.; Moliner, V.; Izzet, G.; Reinaud, O.; Parisel, O. *J. Biol. Inorg. Chem.* **2006**, *11*, 593–608. (u) de la Lande, A.; Gérard, H.; Parisel, O. *Int. J. Quantum Chem.* **2008**, *108*, 1894–1904. (v) Lenci, M. P.; Smirnov, V. V.; Cramer, C. J.; Gauchanova, E. V.; Sundermeyer, J.; Roth, J. P. *J. Am. Chem. Soc.* **2007**, *129*, 14697–14709. (w) Kunishita, A.; Ishimaru, H.; Nakashima, S.; Ogura, T.; Itoh, S. *J. Am. Chem. Soc.* **2008**, *130*, 4244–4245.
- (6) (a) Chen, P.; Solomon, E. I. *J. Am. Chem. Soc.* **2004**, *126*, 4991–5000. (b) Cramer, C. J.; Tolman, W. B. *Acc. Chem. Res.* **2007**, *40*, 601–608.
- (7) Kodera, M.; Kita, T.; Miura, I.; Nakayama, N.; Kawata, T.; Kano, K.; Hirota, S. *J. Am. Chem. Soc.* **2001**, *123*, 7715–7716.

rocyclic monocopper(I) complex and for the subsequent intramolecular alkyl hydroxylation to yield the alkoxide product.

### Computational Details

All geometry optimizations have been performed, without any symmetry constraints, with the *Gaussian03* package,<sup>16</sup> using the B3LYP functional<sup>17</sup> and the standard 6-31G(d) basis set.<sup>18</sup> The geometries obtained at the B3LYP/6-31G(d) level were used to perform single-point energy calculations with a larger basis set, the 6-311G(d,p) basis set, and the same functional [B3LYP/6-311G(d,p)//B3LYP/6-31G(d)]. For copper, the 6-311G(d,p) basis

- (8) (a) Crespo, A.; Martí, M. A.; Roitberg, A. E.; Amzel, L. M.; Estrin, D. A. *J. Am. Chem. Soc.* **2006**, *128*, 12817–12828. (b) Yoshizawa, K.; Kihara, N.; Kamachi, T.; Shiota, Y. *Inorg. Chem.* **2006**, *45*, 3034–3041. (c) Decker, A.; Solomon, E. I. *Curr. Opin. Chem. Biol.* **2005**, *9*, 152–163. (d) Hong, S.; Huber, S. M.; Gagliardi, L.; Cramer, C. C.; Tolman, W. B. *J. Am. Chem. Soc.* **2007**, *129*, 14190–14192. (e) Schröder, D.; Holthausen, M. C.; Schwarz, H. *J. Phys. Chem. B* **2004**, *108*, 14407–14416.
- (9) (a) Karlin, K. D.; Wei, N.; Jung, B.; Kaderli, S.; Niklaus, P.; Zuberbuhler, A. D. *J. Am. Chem. Soc.* **1993**, *115*, 9506–9514. (b) Lee, D.-H.; Wei, N.; Murthy, N. N.; Tyeklár, Z.; Karlin, K. D.; Kaderli, S.; Jung, B.; Zuberbuhler, A. D. *J. Am. Chem. Soc.* **1995**, *117*, 12498–12513. (c) Chaudhuri, P.; Hess, H.; Weyhermüller, T.; Wieghardt, K. *Angew. Chem., Int. Ed.* **1999**, *38*, 1095–1098. (d) Komiya, K.; Furutachi, H.; Nagatomo, S.; Hashimoto, A.; Hayashi, H.; Fujinami, S.; Suzuki, M.; Kitagawa, T. *Bull. Chem. Soc. Jpn.* **2004**, *77*, 59–72. (e) Schatz, M.; Raab, V.; Foxon, S. P.; Brehm, G.; Schneider, S.; Reiher, M.; Holthausen, M. C.; Sundermeyer, J.; Schindler, S. *Angew. Chem., Int. Ed.* **2004**, *43*, 4360–4363. (f) Würtele, C.; Gaoutchenova, E.; Harms, K.; Holthausen, M. C.; Sundermeyer, J.; Schindler, S. *Angew. Chem., Int. Ed.* **2006**, *45*, 3867–3869.
- (10) Maiti, D.; Lee, D.-H.; Gaoutchenova, K.; Würtele, C.; Holthausen, M. C.; Narducci Sarjeant, A. A.; Sundermeyer, J.; Schindler, S.; Karlin, K. D. *Angew. Chem., Int. Ed.* **2008**, *47*, 82–85.
- (11) The labeling is the same as that in ref 7.
- (12) (a) Maiti, D.; Fry, H. C.; Wortink, J. S.; Vance, M. A.; Solomon, E. I.; Karlin, K. D. *J. Am. Chem. Soc.* **2007**, *129*, 264–265. (b) Maiti, D.; Lucas, H. R.; Narducci Sarjeant, A. A.; Karlin, K. D. *J. Am. Chem. Soc.* **2007**, *129*, 6998–6999.
- (13) Güell, M.; Luis, J. M.; Solà, M.; Siegbahn, P. E. M. *J. Biol. Inorg. Chem.* **2009**, *14*, 229–242.
- (14) (a) Herres, S.; Heuwings, A. J.; Florke, U.; Schneider, J.; Henkel, G. *Inorg. Chim. Acta* **2005**, *358*, 1089–1095. (b) Herres-Pawlis, S.; Florke, U.; Henkel, G. *Eur. J. Inorg. Chem.* **2005**, *381*, 3815–3824.
- (15) (a) Becke, A. D. *J. Chem. Phys.* **1993**, *98*, 5648–5652. (b) Lee, C.; Yang, W.; Parr, R. G. *Phys. Rev. B* **1988**, *37*, 785–789. (c) Stevens, P. J.; Devlin, F. J.; Chabalowski, C. F.; Frisch, M. J. *J. Phys. Chem.* **1994**, *98*, 11623–11627.
- (16) Frisch, M. J.; Trucks, G. W.; Schlegel, H. B.; Scuseria, G. E.; Robb, M. A.; Cheeseman, J. R.; Montgomery, J. A.; Vreven, T.; Kudin, K. N.; Burant, J. C.; Millam, J. M.; Iyengar, S. S.; Tomasi, J.; Barone, V.; Mennucci, B.; Cossi, M.; Scalmani, G.; Rega, N.; Petersson, G. A.; Nakatsuji, H.; Hada, M.; Ehara, M.; Toyota, K.; Fukuda, R.; Hasegawa, J.; Ishida, M.; Nakajima, T.; Honda, Y.; Kitao, O.; Nakai, H.; Klene, M.; Li, X.; Knox, J. E.; Hratchian, H. P.; Cross, J. B.; Adamo, C.; Jaramillo, J.; Gomperts, R.; Stratmann, R. E.; Yazyev, O.; Austin, A. J.; Cammi, R.; Pomelli, C.; Ochterski, J. W.; Ayala, P. Y.; Morokuma, K.; Voth, G. A.; Salvador, P.; Dannenberg, J. J.; Zakrzewski, V. G.; Dapprich, S.; Daniels, A. D.; Strain, M. C.; Farkas, Ö.; Malick, D. K.; Rabuck, A. D.; Raghavachari, K.; Foresman, J. B.; Ortiz, J. V.; Cui, Q.; Baboul, A. G.; Clifford, S.; Cioslowski, J.; Stefanov, B. B.; Liu, G.; Liashenko, A.; Piskorz, P.; Komaromi, I.; Martin, R. L.; Fox, D. J.; Keith, T.; Al-Laham, M. A.; Peng, C. Y.; Nanayakkara, A.; Challacombe, M.; Gill, P. M. W.; Johnson, B.; Chen, W.; Wong, M. W.; González, C.; Pople, J. A. *Gaussian03*, revision C02; Gaussian, Inc.: Wallingford, CT, 2004.
- (17) (a) Becke, A. D. *J. Chem. Phys.* **1993**, *98*, 5648–5652. (b) Lee, C.; Yang, W.; Parr, R. G. *Phys. Rev. B* **1988**, *37*, 785–789. (c) Stevens, P. J.; Devlin, F. J.; Chabalowski, C. F.; Frisch, M. J. *J. Phys. Chem.* **1994**, *98*, 11623–11627.
- (18) (a) Hehre, W. J.; Ditchfield, R.; Pople, J. A. *J. Chem. Phys.* **1972**, *56*, 2257–2261. (b) Hehre, W. J.; Radom, L.; Schleyer, P. v. R.; Pople, J. A. *Ab Initio Molecular Orbital Theory*; Wiley: New York, 1986.

set corresponds to the (14s9p5d)/[9s5p3d] Wachters basis set<sup>19</sup> with the contraction scheme 611111111/51111/311 supplemented with one f polarization function. In the *Gaussian03* implementation of the copper basis set, the s and p functions come from Wachters' optimization for the Cu atom in its 2s state, while the d functions come from Wachters' optimization for the Cu atom in its 2d state. The *Gaussian03* internal basis set provides much more reasonable results for the relative energies among the different analyzed states than the basis set does, with the d functions coming from Wachters' optimization for the Cu atom in its 2d state.<sup>20</sup>

Intrinsic reaction pathways were calculated to confirm that the located transition states connected the expected minima. Analytical Hessians were computed to determine the nature of all of the stationary points that we located and to calculate zero-point energies and thermodynamic properties at 298 K, at the B3LYP/6-31G(d) level at 298 K.<sup>21</sup>

For open-shell states, the geometry optimizations were performed within the broken-symmetry unrestricted methodology, while for the closed-shell singlet states, the restricted formalism was used. Theoretical treatment of biradical singlet species requires multi-configurational or multireference methods due to strong static electron correlation. Unfortunately, these methods can only be applied to relatively small systems because computationally they are extremely demanding. As an alternative, we have used the unrestricted UB3LYP method in broken symmetry (using GUESS = MIX).<sup>22</sup> This method improves the modeling of biradical singlet states at the expense of introducing some spin contamination from higher spin states.<sup>23,24</sup> Although this is not the most appropriate method to treat biradical singlet species, it has been shown that it can be used provided that the overlap between the open-shell orbitals is small (i.e., the unpaired electrons are located in separated atomic centers), which is the case of the systems that show predominant biradical character in this work.<sup>23g</sup> In a previous paper, for *p*-benzyne, the application of the sum rule<sup>23f</sup> to the energy of the biradical singlet state to remove the spin-contamination error does not improve the calculated singlet–triplet energy gap but rather leads to larger errors when compared to the experimental value.<sup>22</sup> For this reason, open-shell singlet energies reported in this work do not contain spin-contamination corrections.

Solvent effects including contributions of nonelectrostatic terms have been estimated in single-point calculations on the gas-phase optimized structures, based on the polarizable continuum solvation

- (19) Wachters, A. J. H. *J. Chem. Phys.* **1970**, *52*, 1033–1036.
- (20) Güell, M.; Luis, J. M.; Rodríguez-Santiago, L.; Sodupe, M.; Solà, M. *J. Phys. Chem. A* **2008**, *113*, 1308–1317.
- (21) (a) Poater, A.; Gallegos-Saliner, A.; Carbó-Dorca, R.; Poater, J.; Solà, M.; Cavallo, L.; Worth, A. P. *J. Comput. Chem.* **2008**, *30*, 275–284. (b) Gallegos-Saliner, A.; Poater, A.; Worth, A. P. *IDRUGS* **2008**, *11*, 728–732.
- (22) Caballo, R.; Castell, O.; Illas, F.; Moreira, I. d. P. R.; Malrieu, J. P. *J. Phys. Chem. A* **1997**, *101*, 7860–7866.
- (23) (a) Winkler, M. *J. Phys. Chem. A* **2005**, *109*, 1240–1246. (b) Lindh, R.; Bernhardsson, A.; Schütz, M. *J. Phys. Chem. A* **1999**, *103*, 9913–9920. (c) Cramer, C. J. *J. Chem. Soc., Perkin Trans. 2* **1999**, 2273–2283. (d) Kikuchi, A.; Ito, H.; Abe, J. *J. Phys. Chem. B* **2005**, *109*, 19448–19453. (e) Borden, W. T. Diradicals. In *The Encyclopedia of Computational Chemistry*; Schleyer, P. v. R., Allinger, N. L., Clark, T., Gasteiger, J., Kollman, P. A., Schaeffer, H. F., III, Eds.; John Wiley & Sons: Chichester, U.K., 1998; pp 708–722. (f) Poater, J.; Bickelhaupt, F. M.; Solà, M. *J. Phys. Chem. A* **2007**, *111*, 5063–5070. (g) Gräfenstein, J.; Kraka, E.; Filatov, M.; Cremer, D. *Int. J. Mol. Sci.* **2002**, *3*, 360–394.
- (24) Borden, W. T.; Davidson, E. R. *Acc. Chem. Res.* **1996**, *29*, 67–75.

model using CH<sub>3</sub>CN as a solvent. The solvent effect was introduced by the conductor polarizable calculation model.<sup>25</sup> The cavity is created via a series of overlapping spheres.

The relative free energies reported in this work include energies computed at the B3LYP/6-311G(d,p)//B3LYP/6-31G(d) level of theory together with solvent effects.

## Results and Discussion

Initially, the interaction of the [Cu<sup>1</sup>(TMG<sub>3</sub>tren)]<sup>+</sup> complex with one CH<sub>3</sub>CN solvent molecule was investigated. However, formation of the [Cu<sup>1</sup>(TMG<sub>3</sub>tren)]<sup>+</sup>/CH<sub>3</sub>CN adduct from the separated species is unfavored by 1.8 kcal·mol<sup>-1</sup>, probably because of repulsive steric interaction with the bulky (TMG<sub>3</sub>tren) ligand. For this reason, we decided to start the reaction pathway from interaction of the free [Cu<sup>1</sup>(TMG<sub>3</sub>tren)]<sup>+</sup> complex in the singlet electronic state with a free O<sub>2</sub> molecule to form the superoxide complex **1** of Figure 1. The calculations suggest a barrierless approach of the O<sub>2</sub> molecule to the Cu atom. In complex **1**, the Cu–O interaction can be characterized as a typical end-on superoxo coordination. The O–O distance is 1.302 Å and the O–O stretching frequency is 1235.0 cm<sup>-1</sup>, thus displaying the typical parameters of end-on triplet structures.<sup>5t</sup> Overall, the geometry of **1** that we calculated is in excellent agreement with the X-ray structure (rmsd = 0.024 Å on distances and 1.0° on angles).<sup>26</sup> As in previous similar studies,<sup>27</sup> the density functional theory (DFT) approach that we choose, i.e., B3LYP/6-311G(d,p)//B3LYP/6-31G(d) level of theory, can offer reliable insight on the geometry of other intermediates along the reaction path, for which no X-ray data are available. We also tried to locate a geometry corresponding to a side-on peroxo coordination, but all of the attempts collapsed into the end-on superoxo species **1**. The electronic ground state of **1** corresponds to a triplet, although the biradical singlet (with a  $\langle S^2 \rangle$  of 1.005) is competitive in energy because it is only 2.6 kcal·mol<sup>-1</sup> above that of **1**. Differently, the closed-shell singlet is far higher in energy (21.5 kcal·mol<sup>-1</sup> above

- (25) (a) Barone, V.; Cossi, M. *J. Phys. Chem. A* **1998**, *102*, 1995–2001. (b) Tomasi, J.; Persico, M. *Chem. Rev.* **1994**, *94*, 2027–2094.
- (26) Standard deviations for distances and angles:  $s_{n-1} = [\sum_{i=1}^N (CV - EV)^2 / (N - 1)]^{1/2}$ , where CV means calculated value, EV means experimental value (X-ray data), and N is the number of distances or angles taken into account (distances and angles used are given in Table S2 of the Supporting Information). For examples, see: (a) Duran, J.; Polo, A.; Real, J.; Benet-Buchholz, J.; Poater, A.; Solà, M. *Eur. J. Inorg. Chem.* **2003**, *414*, 4147–4151. (b) Sala, X.; Poater, A.; von Zelewsky, A.; Parella, T.; Fontrodona, X.; Romero, I.; Solà, M.; Rodríguez, M.; Llobet, A. *Inorg. Chem.* **2008**, *47*, 8016–8024. (c) Mola, J.; Rodríguez, M.; Romero, I.; Llobet, A.; Parella, T.; Poater, A.; Solà, M.; Benet-Buchholz, J. *Inorg. Chem.* **2006**, *45*, 10520–10529. (d) Sala, X.; Plantalech, E.; Romero, I.; Rodríguez, M.; Llobet, A.; Poater, A.; Duran, M.; Solà, M.; Jansat, S.; Gómez, M.; Parella, T.; Stoeckli-Evans, H.; Benet-Buchholz, J. *Chem.—Eur. J.* **2006**, *12*, 2798–2807. (e) Costas, M.; Ribas, X.; Poater, A.; López-Valbuena, J. M.; Xifra, R.; Company, A.; Duran, M.; Solà, M.; Llobet, A.; Corbella, M.; Usón, M. A.; Mahía, J.; Solans, X.; Shan, X.; Benet-Buchholz, J. *Inorg. Chem.* **2006**, *45*, 3569–3581. (f) Poater, A.; Mola, J.; Gallegos-Saliner, A.; Romero, I.; Rodríguez, M.; Llobet, A.; Solà, M. *Chem. Phys. Lett.* **2008**, *458*, 200–204. (g) Mola, J.; Romero, I.; Rodríguez, M.; Bozoglian, F.; Poater, A.; Solà, M.; Parella, T.; Benet-Buchholz, J.; Fontrodona, X.; Llobet, A. *Inorg. Chem.* **2007**, *46*, 10707–10716. (h) Poater, A.; Moradell, S.; Pinilla, E.; Poater, J.; Solà, M.; Martínez, M. A.; Llobet, A. *Dalton Trans.* **2006**, 1188–1196.
- (27) (a) Poater, A.; Ribas, X.; Llobet, A.; Cavallo, L.; Solà, M. *J. Am. Chem. Soc.* **2008**, *130*, 17710–17717. (b) Poater, A.; Cavallo, L. *Inorg. Chem.* **2009**, *48*, 2340–2342.

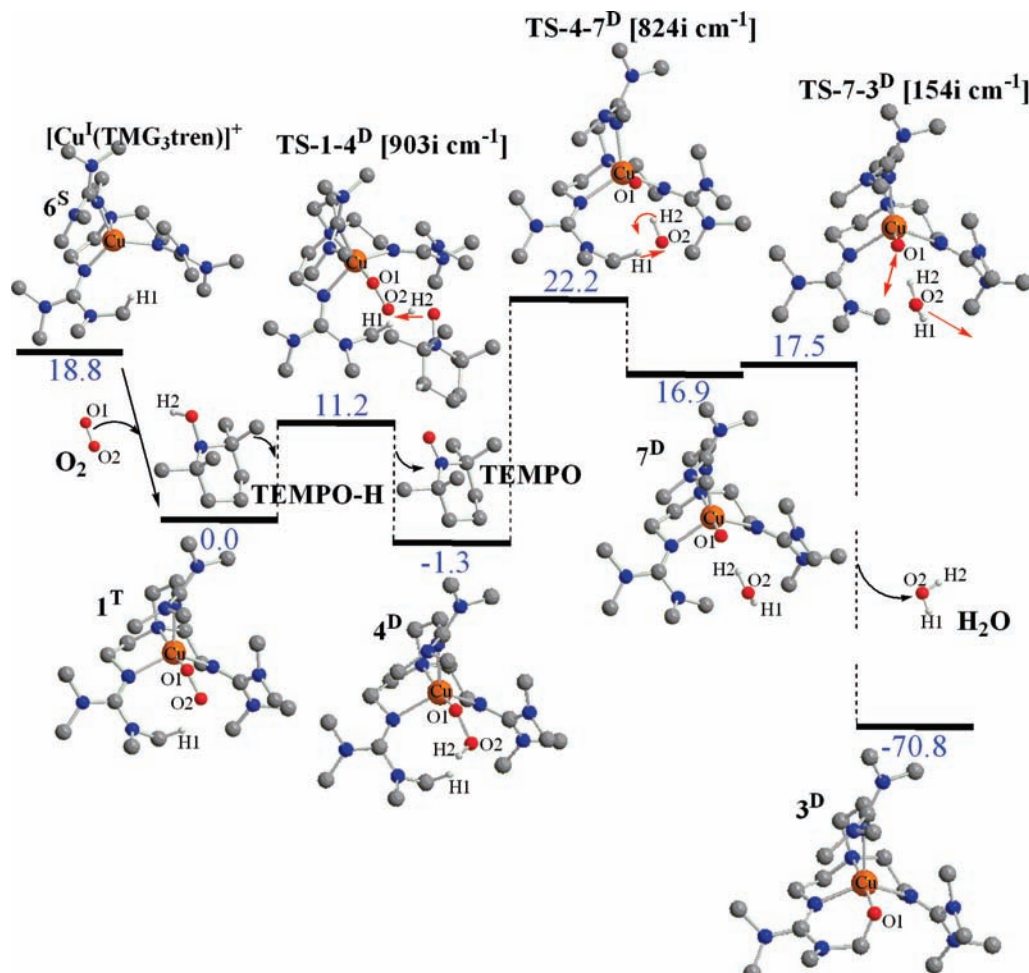


**Figure 1.** Stationary points located for the reaction mechanism that leads to complex **3** (most H atoms are omitted for the sake of clarity), with free energies relative to complex **1<sup>T</sup>** (in  $\text{kcal}\cdot\text{mol}^{-1}$ ) in solution. Calculated imaginary frequencies for transition structures are given in brackets. Superindexes S (closed-shell singlet), D (open-shell doublet), and T (triplet) refer to the multiplicity of the ground state.

that of **1**). Incidentally, for the closed-shell singlet, we were able to locate a side-on peroxo coordination, instead of the end-on coordination, although this side-on peroxo coordination is 24.0  $\text{kcal}\cdot\text{mol}^{-1}$  higher in energy than that of **1<sup>T</sup>**.

Abstraction of a H atom from TEMPO-H leads to the Cu<sup>II</sup>OOH hydroperoxo species **4** with a barrier of only 11.2  $\text{kcal}\cdot\text{mol}^{-1}$ . The electronic ground state of **4** is a doublet, and the H<sup>+</sup> transfer from TEMPO-H to **1** is exoergic by 1.3  $\text{kcal}\cdot\text{mol}^{-1}$ . Complex **4** has a weaker O–O bond with respect to **1** (1.460 vs 1.302 Å), which reinforces the Cu–O bond (1.882 vs 1.924 Å).<sup>10</sup>

Activation by the Cu<sup>II</sup>OOH moiety of a C–H bond of one of the N-bonded methyl groups close to the copper expels a water molecule and leads to the high-energy intermediate **7**, 16.9  $\text{kcal}\cdot\text{mol}^{-1}$  above that of **1** + TEMPO-H, with a barrier of 23.5  $\text{kcal}\cdot\text{mol}^{-1}$ . In the course of the reaction, the exiting OH group rotates by almost 180°, so that the very late **4**–**7** transition state is stabilized by a H-bond between the exiting OH group and the O atom of the Cu–O group. This H-bond is held in place also in complex **7**. The electronic ground state of **7** is a doublet, and natural population analysis indicates that spare  $\alpha$  electrons are mostly located on the activated oxyl species (O1) and on the Cu atom, with a Mulliken spin density of 1.07e and 0.67e, respectively, while

on the radical CH<sub>2</sub><sup>•</sup> moiety, there is a  $\beta$  spin density of 0.83e. For this species, the quadruplet is placed only 0.1  $\text{kcal}\cdot\text{mol}^{-1}$  above in energy, with an almost identical structure. Electronically, this change in the electronic state corresponds to a change in the spin density mostly located on the radical CH<sub>2</sub><sup>•</sup> moiety from  $\beta$  to  $\alpha$ .

The high-energy complex **7** collapses to complex **3** with the kinetically irrelevant barrier of 0.6  $\text{kcal}\cdot\text{mol}^{-1}$ , with complete expulsion of the water molecule and concomitant formation of the O–C bond of **3**. The overall **1** + TEMPO-H to **3** + H<sub>2</sub>O transformation is exoergic by 70.8  $\text{kcal}\cdot\text{mol}^{-1}$ . The electronic ground state of **3** also is a doublet, so that after H<sup>+</sup> transfer from TEMPO-H (or any other substrate) to **1** to form **4**, the reaction proceeds on the doublet electronic state. Again, we found a good agreement between the DFT and the X-ray structure of **3** (rmsd = 0.038 Å on distances and 1.6° on angles), which supports our geometrical analysis of intermediate **4**. After studying the quartet electronic state of **7**, we did not investigate its reactivity because the C–O bond closure from this electronic state is not possible.<sup>28</sup>

Considering the debate on which is the most suitable DFT to describe the low-lying electronic states of Cu–O

(28) Schröder, D.; Shaik, S.; Schwarz, H. *Acc. Chem. Res.* **2000**, *33*, 139–145.

complexes,<sup>5i,29</sup> we tested our conclusions with the pure BLYP functional. As expected, the absolute energetics are somewhat different, but most important is the fact that the relative energies are substantially the same, which indicates that the chemical scenario that we described is rather independent of the specific computational method.<sup>30</sup> For example, the energetic difference between **1<sup>S</sup>** and **1<sup>T</sup>** is 4.7 kcal·mol<sup>-1</sup>, however also favoring the triplet multiplicity. We must point out that all attempts performed for spin-unrestricted broken-symmetry calculations for the singlet diradical state with BLYP, starting from unsymmetrical wave functions, have reconverged to the restricted solution. On the other hand, we investigated other possible routes from **1** to **3**, but they were discarded because of the unfavorable energetics. For example, we examined if the H atom from the donor species (TEMPO-H) could be transferred to the O atom that is bonded to Cu atom. However, this isomer, complex **8** displayed in Figure 2, is 16.7 kcal·mol<sup>-1</sup> less stable in energy with respect to complex **4**. On the other hand, we considered a mechanism starting from **4** where the C atom attacks O1 prior to the H-atom abstraction; however, this route was found to be not feasible. Moreover, we also investigated an alternative path from **1**, which does not involve transfer of a H atom from TEMPO-H. This alternative pathway involves the donation of one H atom from one of the methyl groups to the Cu—O—O moiety. This transition state, **TS-1-9** in Figure 2, requires to overcome a barrier of 26.7 kcal·mol<sup>-1</sup>, which is remarkably higher than the barrier corresponding to H donation by TEMPO-H. Therefore, the cleavage of a C—H bond of one of the methyl groups is not favored with respect to donation from a H donor such as TEMPO-H. This is different from a recent study on a very strictly related copper complex where, in the absence of an external H donor, intramolecular H transfer from a C—H or a N—H bond was found to be possible.<sup>5s</sup> The minimum that is reached from transition state **TS-1-9**, species **9**, presents a stable Cu<sup>II</sup>OOH core, but it is destabilized by the formation

(29) (a) Lewin, J. L.; Heppner, D. E.; Cramer, C. J. *J. Biol. Inorg. Chem.* **2007**, *12*, 1221–1234. (b) Cramer, C. J.; Włoch, M.; Piecuch, P.; Puzzarini, C.; Gagliardi, L. *J. Phys. Chem. A* **2006**, *10*, 1991–2004.

(c) Gherman, B. F.; Cramer, C. J. *Coord. Chem. Rev.* **2009**, *293*, 723–753.  
 (30) (a) Siegbahn, P. E. M. *J. Biol. Inorg. Chem.* **2003**, *8*, 577–585. (b) Güell, M.; Siegbahn, P. E. M. *J. Biol. Inorg. Chem.* **2007**, *12*, 1251–1264. (c) Company, A.; Lamata, D.; Poater, A.; Solà, M.; Rybak-Akimova, E.; Que, L., Jr.; Fontrodona, X.; Parella, T.; Llobet, A.; Costas, M. *Inorg. Chem.* **2006**, *45*, 5239–5241. (d) Company, A.; Gómez, L.; Mas-Ballesté, R.; Korendovych, I. V.; Ribas, X.; Poater, A.; Parella, T.; Fontrodona, X.; Benet-Buchholz, J.; Solà, M.; Que, L., Jr.; Rybak-Akimova, E.; Costas, M. *Inorg. Chem.* **2007**, *46*, 4997–5012.

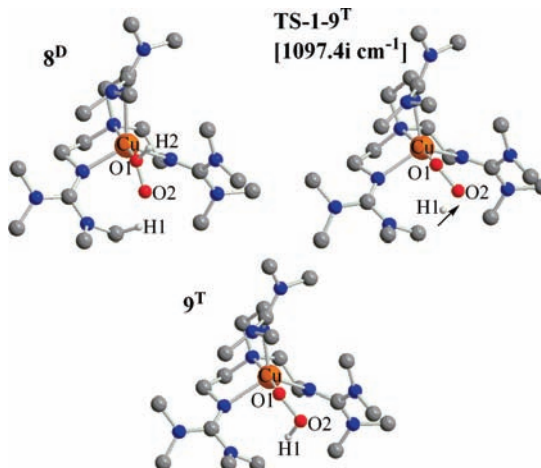


**Figure 2.** Alternative stationary points located for the reaction mechanism leading to complex **3** (most H atoms are omitted for the sake of clarity). Calculated imaginary frequencies for transition structures are given in brackets. Superindex D (open-shell doublet), and T (triplet) refer to the multiplicity of the ground state.

of a radical CH<sub>2</sub><sup>•</sup> group, which explains why **9** is 23.5 kcal·mol<sup>-1</sup> less stable than **1**.

## Conclusions

In summary, our calculations are completely consistent with the key hypothesis of Karlin et al. that hydroperoxo complexes, such as [Cu<sup>II</sup>(TMG<sub>3</sub>tren)OOH]<sup>+</sup>, are the fundamental intermediate in the C—H hydroxylation reaction promoted by Cu—O complexes and thus constitute an additional piece toward the full understanding of a class of reaction of biological relevance. Further, the lack of high-energy barriers and deep energy wells along the reaction pathway explains the experimental difficulties in trapping other intermediates. The rate-limiting step is the H-atom abstraction of the methyl that takes place after the role of an external H donor as TEMPO-H.

**Acknowledgment.** We thank Prof. M. Solà for helpful discussion, the Generalitat de Catalunya for a Beatriu de Pinós postdoctoral fellowship to A.P., and the INSTM-Italy for a CINECA Key-Project Grant.

**Supporting Information Available:** Complete computational methods, Cartesian coordinates, and drawings of all of the stationary points located. This material is available free of charge via the Internet at <http://pubs.acs.org>.

IC802269V